

1 **Mitigation of nitrogen pollution in vegetated ditches fed by nitrate-rich spring**  
2 **waters**

3

4 Elisa Soana<sup>1</sup>, Raffaella Balestrini<sup>2</sup>, Fabio Vincenzi<sup>1</sup>, Marco Bartoli<sup>3\*</sup>, Giuseppe Castaldelli<sup>1</sup>

5 1. Department of Life Sciences and Biotechnology, University of Ferrara, Via L. Borsari 46 - 44121  
6 Ferrara – Italy

7 2. Water Research Institute, National Research Council (IRSA-CNR), Via del Mulino 19 - 20861  
8 Brugherio, MB – Italy

9 3. Department of Chemistry, Life Sciences and Environmental Sustainability, University of Parma,  
10 Viale G.P. Usberti 33/A - 43124 Parma – Italy

11 \*Corresponding author: [marco.bartoli@unipr.it](mailto:marco.bartoli@unipr.it)

12 **Abstract**

13 In permeable soils, excess nitrate from agriculture is transported vertically and accumulates in  
14 aquifers. However, it can come back to the surface via groundwater movement and pollute  
15 watercourses. We hypothesized that vegetated ditches may dissipate significant amounts of nitrate  
16 from spring waters, and represent a buffer system to protect downstream water bodies from  
17 eutrophication. To test this hypothesis, nitrate removal was measured in ditches fed by nitrate-rich  
18 groundwater in presence and absence of emergent vegetation. Reach-scale methods ( $N_2$  open-  
19 channel, N budgets) were coupled with laboratory incubations of sediment cores (benthic N fluxes,  
20 isotope pairing) and plant N uptake estimation. Studied ditches are representative of a wide  
21 hydrological network in Northern Italy, within the so-called “spring-belt” (Po River plain), a  $NO_3^-$ -  
22 vulnerable area with high density of contaminated springs.

23 Results indicated a greater reach-scale N removal in vegetated ( $38-84 \text{ mmol N m}^{-2} \text{ d}^{-1}$ ) as compared  
24 to unvegetated condition ( $12-45 \text{ mmol N m}^{-2} \text{ d}^{-1}$ ). Denitrification was the dominant N-removal  
25 pathway, while plant uptake represented a minor fraction of the net N abatement. Large development  
26 of interfaces for microbial growth provided by aquatic vegetation and more opportunities for biotic  
27 interactions are features that promote nitrate reduction in the ditch network. Despite the vegetated  
28 ditches were significant N-reactors, denitrification provided a little N-removal to in-stream high  
29 nitrate loads, with the exception of periods when plant coverage and water retention time peaked.  
30 Management of N-saturated ditches may consist in the enlargement of stretches to increase water  
31 retention and amplify the interfaces where biofilms develop, though preserving hydraulic efficiency.  
32 The maintenance of vegetation in the ditch networks would result in a significant N-abatement on a  
33 larger scale.

34

35 **Keywords**

36 Ditch network; nitrate pollution; springs; vegetation; denitrification;  $N_2$  open-channel method

## 37        **1. Introduction**

38        In the last century, the intensification of agricultural activities and soil loss due to urbanization have  
39        deeply simplified the landscape in lowland areas, by removing natural habitats as wetlands and  
40        riparian vegetated zones (Groffman et al., 2003; Hefting et al., 2014). These human-impacted  
41        watersheds have lost their capacity to buffer excess nutrient loads, whose delivery to coastal waters  
42        is further accelerated by river morphological alterations such as channelization, burial, and water  
43        withdrawal, and by decreased connectivity between riverbeds and floodplains (Roley et al., 2012;  
44        Beaulieu et al., 2015). Modern agriculture has further modified the landscape through the  
45        implementation of extensive artificial canal networks, dug ex novo for wetland reclamation or  
46        resectioned in former natural river networks. In both cases, they often constitute a capillary network  
47        arranged to maximize multiple water uses, as drainage and irrigation, and have become integral  
48        components and ubiquitous features of many productive agro-ecosystems (Pierce et al., 2012;  
49        Dollinger et al., 2015).

50        Small-size watercourses, no matter if natural or artificial, are the interfaces between agricultural lands  
51        and downstream aquatic ecosystems, such as rivers, estuaries or lagoons and coastal waters. Such  
52        canals are characterized by multiple interfaces between water, sediment and aquatic vegetation  
53        (Marion et al., 2014; Pinay et al., 2015). Here, nitrogen (N) removal takes place as a result of several  
54        plant and microbially-mediated N transformations, among which the dominant are assimilation and  
55        denitrification, the reduction of nitrate ( $\text{NO}_3^-$ ) to N gases under anaerobic conditions (Schaller et al.,  
56        2004; Bernot and Dodds, 2005, Mulholland et al., 2008). Small canals and ditches can contribute  
57        significantly to watershed N dynamics because of their capillary distribution and high metabolic  
58        capacity. The latter is sustained by the high ratio between bio-reactive surfaces, directly or indirectly  
59        ascribable to aquatic macrophytes, and water volumes (Marion et al., 2014; Srivastava et al., 2016).  
60        Recent studies have suggested a new perspective on the role of canal networks in watershed N  
61        dynamics by proving that agricultural basins can generate large N excess but little export (Bartoli et

62 al., 2012; Castaldelli et al., 2013; Romero et al., 2016). Interest has grown on the identification and  
63 parametrization of landscape elements that provide high rates of N removal. However, the debate is  
64 still open if intensively cultivated systems may maintain or not these relevant ecosystem functions,  
65 since aquatic vegetation is generally considered an impediment for water circulation and  
66 mechanically removed during routine management practices of ditches (Duncan et al., 2013; Pinay  
67 et al., 2015).

68 While many studies have investigated N removal in wetlands and afforested riparian zones (e.g.  
69 Balestrini et al., 2008; Tournebize et al., 2017), the process is understudied in ditches and canals  
70 (Pierobon et al., 2013; Taylor et al., 2015; Balestrini et al., 2016; Iseyemi et al., 2016). Although there  
71 are profound implications for the re-establishment of beneficial ecosystem services in agricultural  
72 basins with extensive water networks, only a few studies provided field experimental data on N  
73 dynamics in ditches suitable to upscaling at the watershed level (e.g. Birgand et al., 2007; Castaldelli  
74 et al., 2015). Conventional methods applied on intact sediment cores (i.e. isotope pairing technique;  
75 Nielsen 1992) give precise estimates of denitrification rates but cannot be used to infer about  
76 processes in lotic environments where multiple riverine habitats and interfaces exist (e.g. sediments  
77 with irregular associations of submerged and/or emergent macrophytes). The N<sub>2</sub> open-channel  
78 method provides direct whole-system estimates of denitrification in running waters derived from  
79 accurate measurements of N<sub>2</sub> concentrations in a conceptual moving parcel of water while accounting  
80 for gas exchanges with the atmosphere. This methodology integrates small-scale spatial and temporal  
81 variability in processes and overcomes the limitations inherent in the upscaling of results from the  
82 laboratory to the field (e.g. measurements performed over small surfaces, incubation artifacts, etc.).  
83 Further, this method quantifies denitrification under natural conditions at spatial and temporal scales  
84 appropriate to assess its relevance to watershed N fluxes modelling and management (Gardner et al.,  
85 2016; Reisinger et al., 2016). Eventually, the net effect of vegetation on in-stream N metabolism can  
86 be discriminated if two conditions (vegetated and unvegetated) are compared, and the multiple N  
87 pathways can be disentangled if several methods are concomitantly applied (Castaldelli et al., 2015).

88 The aim of the present study was to quantify N removal in ditches fed by spring water contaminated  
89 by  $\text{NO}_3^-$ , in the presence and absence of emergent vegetation and along its growth cycle. Studied  
90 ditches belong to the “spring-belt”, an area of the Po valley (Northern Italy) where groundwater  
91 interacts with surface waters due to many permanent man-modified resurgences, locally known as  
92 “*fontanili*”, originating from changes in slope profile and soil permeability. Here,  $\text{NO}_3^-$ -contaminated  
93 groundwater may pollute rivers, canals, ditches and downstream water bodies, if  $\text{NO}_3^-$  is not  
94 intercepted (Laini et al., 2011; Sacchi et al., 2013; Viaroli et al., 2015). In this study, denitrification  
95 rates estimated in ditches by the  $\text{N}_2$  open-channel method were compared to reach-scale budgets of  
96 inorganic N species and to benthic N fluxes measured by sediment core incubations, according to an  
97 experimental protocol previously validated for similar watercourses in the lower portion of the Po  
98 River basin (Castaldelli et al., 2015). As  $\text{NO}_3^-$  availability from the groundwater feeding the ditch  
99 network is always not limiting and almost constant during the year, we hypothesize high  
100 denitrification rates and emergent vegetation as the primary control on in-stream N dynamics, by  
101 sustaining quantitatively relevant microbial processes responsible for N removal. In fact, under N  
102 excess the competition between uptake by primary producers and microbial denitrification is  
103 smoothed and high rates of both processes can simultaneously occur (Soana et al., 2015; Racchetti et  
104 al., in press).

105 Results from this and other similar studies may define appropriate management practices of ditches  
106 and canals, targeting  $\text{NO}_3^-$  removal. In the development of the hydrological network, from small  
107 waterways to large and deep canals, shallow ditches represent the level at which it is possible to  
108 operate effective management practices, avoiding hydrological risks and economically unsustainable  
109 investments. The hypothesis of intervention implies the recovery of dense vegetation stands in  
110 suitable stretches, to enhance  $\text{NO}_3^-$  removal.

111

## 112 2. Material and Methods

## 113 2.1 Study area and experimental approach

114 The study was carried out in two ditches, V (with in-stream vegetation) and U (without in-stream  
115 vegetation), located in the eastern part of the Metropolitan City of Milan (Lombardy Region, Northern  
116 Italy). The two sites belong to the central, flat, agricultural plain of the Po River watershed, within  
117 the Lambro River sub-basin (Fig. 1). This territory is highly urbanized and industrialized, but large  
118 portions still host agricultural lands, crossed by dense networks of artificial canals and ditches, built  
119 over the course of centuries for drainage and irrigation purposes. The two ditches (V: 45°27'25.78"N,  
120 9°24'59.23"E; and U: 45°27'25.21"N, 9°24'47.91"E) are adjacent, similar in length, uniform in  
121 morphology and without any lateral surface water input or output along the studied stretches (Fig.1,  
122 Table 1). They are fed by NO<sub>3</sub><sup>-</sup>-rich groundwater, originating from the same spring named “Quattro  
123 Ponti” (Fig.1; Table 1) and are representative of this territory, where many springs feed steadily a  
124 dense hydrological network of ditches and canals although with seasonal variations of discharge  
125 (Laini et al., 2011). The fields surrounding the two investigated sites, cultivated with maize, affected  
126 ditch flow only during extremely heavy rain events, which anyway did not take place during sampling  
127 periods.

128 Macrophyte coverage at V was persistent over the three sampling dates and included the emergent  
129 reed canary-grass *Typhoides arundinacea* L. Moench (syn *Phalaris arundinacea* L.) and some  
130 submerged species, among which *Elodea canadensis* was the most widespread. As described  
131 afterwards in section 2.3, species-specific coverage was measured only for the dominant species, *T.*  
132 *arundinacea*, whose biomass accounted on average >90% of the total plant biomass along the studied  
133 stretch in all samplings. At the end of the growing season, after the crop harvest on the nearby fields,  
134 the local water authority makes a vegetation mowing, usually in October. U is bordered by a narrow  
135 riparian strip (< 4 m) on both sides consisting of hardwoods, mostly oaks (*Quercus robur*) and elms  
136 (*Ulmus* sp.). The presence of the canopy naturally hampers the development of in-stream aquatic  
137 vegetation. Coarse particulate organic matter and woody debris are randomly present in the ditch bed.  
138 At both sites, phytoplankton is not a relevant primary producer (chlorophyll-*a* <0.5 µg L<sup>-1</sup>).

139 Three sampling campaigns were carried out in May, July, and September 2014, during stable  
140 hydrological and meteorological conditions and with no effect of rainfalls. Samplings were performed  
141 in the dark and in the light, from 02:30 a.m. to 05:30 a.m. and from 01:30 p.m. to 04:30 p.m.,  
142 respectively. The experimental programme was planned to cover three key stages of the plant growth  
143 cycle, namely the spring growth phase, the summer areal coverage peak, and the maturity phase at  
144 the end of summer. Two sampling stations (upstream and downstream) were selected on each ditch,  
145 and three experimental approaches were applied: 1) N<sub>2</sub> open-channel method; 2) reach-scale balance  
146 of inorganic N species and, 3) incubation of bare sediment cores. Methods 1) and 2) were applied  
147 both in the dark and light phase to discriminate the effect of photosynthetic processes on N  
148 metabolism. Finally, for V, N uptake by in-stream vegetation was calculated by areal coverage,  
149 growth rates and biomass elemental composition, and compared to the reach-scale balance of N  
150 species.

151

## 152 2.2 N<sub>2</sub> open-channel method

153 Reach-scale denitrification was modelled according to the method proposed by Laursen and  
154 Seitzinger (2002). The approach provides the direct estimate of the process by measuring the variation  
155 of the end-product N<sub>2</sub> in a parcel of water as it moves downstream, from the N<sub>2</sub>:Ar ratio analysed by  
156 Membrane Inlet Mass Spectrometry (MIMS). A model-based approach is used to solve for  
157 denitrification rates, correcting the variations of N<sub>2</sub> for re-aeration during downstream transport. Both  
158 N<sub>2</sub> and Ar concentrations are assumed to change during downstream transport as a function of re-  
159 equilibration with the atmosphere, and for N<sub>2</sub> also as a function of microbial activity. Denitrification  
160 is estimated based on the production rate required to explain the excess N<sub>2</sub>, namely the measured  
161 change not accounted for by atmospheric exchanges. This approach allows for the calculation of *in*  
162 *situ* net N<sub>2</sub> fluxes (i.e. total denitrification, including coupled nitrification/denitrification, minus N<sub>2</sub>  
163 fixation) at a reach-scale, where accurate NO<sub>3</sub><sup>-</sup> mass balances can be also performed.

164 The selected ditches were sampled from access points using a Lagrangian two-stations (upstream and  
165 downstream) approach. Water samples for dissolved N<sub>2</sub> analyses were collected from the same water  
166 parcel as it moved downstream. Mean velocity and travel time of the water parcel between the two  
167 sampling locations were calculated from the wet section area and discharge. Depth was measured at  
168 equally spaced vertical transects, from a minimum of 6 to a maximum of 10 depending upon the ditch  
169 width. Water velocity was measured in a grid of points along the ditch sections, typically every 0.5  
170 and 0.1 m along the horizontal and vertical axes, respectively, by means of a current meter (Open  
171 Stream CurrentMeter 2100) mounted on a measuring pole with centimetric resolution, equipped with  
172 a modified propeller for low flow conditions. Data were then integrated to calculate ditch discharge  
173 by means of the software Surfer® 11 (Golden Software, LLC). This procedure was replicated at  
174 multiple cross sections, three at least, for each ditch and average discharge was obtained.

175 Water temperature, oxygen and conductivity were measured with a multiparametric probe (Ocean  
176 Seven, 316, Idronaut, Italy). Samples for N<sub>2</sub>:Ar were withdrawn in triplicate directly from the ditches  
177 using a glass syringe and transferred into 12-mL glass-tight vials (Exetainer, Labco, High Wycombe,  
178 UK), flushing at least 3 times the vial volume and preserved by adding 100 µL of ZnCl<sub>2</sub> saturated  
179 solution. The N<sub>2</sub>:Ar ratio in water samples was measured using a MIMS (Bay Instruments, Easton,  
180 MD; Kana et al., 1994) at the laboratory of Aquatic Ecology, University of Ferrara. The coefficient  
181 of variation calculated from replicated N<sub>2</sub>:Ar samples (n=10) was 10-fold lower (~0.04%) than N<sub>2</sub>  
182 measurements (~0.4%), in accordance to Laursen and Seitzinger (2002). N<sub>2</sub> concentration was  
183 calculated from the measured N<sub>2</sub>:Ar multiplied by the equilibrium Ar concentration at the *in situ*  
184 water temperature, determined from the solubility equation (Weiss, 1970; Taylor et al., 2015).

185 Net N<sub>2</sub> fluxes at the reach scale were simulated at 1-min time steps by providing the following model  
186 input parameters: measured N<sub>2</sub> concentrations and water temperature at upstream and downstream  
187 stations, average depth and width, gas transfer velocity (k<sub>600</sub>), Schmidt number coefficient (2/3 for  
188 surfaces without waves; Jähne et al., 1987), and travel time of the water parcel from upstream to  
189 downstream, calculated from average current velocity (Laursen and Seitzinger, 2002). If the ratio of



190 stream velocity to stream depth is higher than  $0.03 \text{ s}^{-1}$ , benthic turbulence is considered the primary  
191 driver of gas exchanges (Schwarzenbach et al., 1993). As this criterion was fulfilled for the  
192 investigated reaches, the oxygen reaeration coefficient ( $K_{O_2}$ ,  $20^\circ\text{C}$ ,  $\text{d}^{-1}$ ) was calculated by means of  
193 a set of empirical equations (Haider et al., 2013), which use average current velocity and water depth  
194 as the only variables affecting reaeration. The transfer velocity for oxygen ( $k_{O_2}$ ,  $20^\circ\text{C}$ ,  $\text{cm h}^{-1}$ ) was  
195 obtained by multiplying each reaeration coefficient by the correspondent water depth, assuming a  
196 well-mixed water column, and finally normalized to a Schmidt number of 600 ( $k_{600}$ , for  $\text{CO}_2$  at  $20$   
197  $^\circ\text{C}$ ,  $\text{cm h}^{-1}$ ) (Jähne et al., 1987; Wanninkhof, 1992). A conservative approach was adopted in this  
198 study, as a set of depth–velocity equations was applied with the aim of providing a range of  $k_{600}$   
199 values, likely including the true value of each investigated ditch (Laini et al., 2011; Castaldelli et al.,  
200 2015). Simulations were run by varying the gas transfer parameterizations and a range of  $\text{N}_2$   
201 production rates was obtained for each reach in each sampling period. The upstream–downstream  
202 balance of inorganic N species sets a limit to the minimum in-stream N removal and the comparison  
203 to the  $\text{N}_2$  open-channel method helped to identify the more realistic reaeration coefficient for each  
204 system. Hourly rates ( $\text{mmol N m}^{-2} \text{ h}^{-1}$ ) were multiplied by the correspondent number of light and dark  
205 hours in each of the three investigated months (15, 16, 13 hours of light in May, July, and September,  
206 respectively) and summed to obtain daily values ( $\text{mmol N m}^{-2} \text{ d}^{-1}$ ).

### 207 208 *2.3 Reach-scale inorganic N mass balance and N uptake by vegetation*

209 Samples for dissolved inorganic N (DIN) as sum of  $\text{NO}_3^-$ , nitrite ( $\text{NO}_2^-$ ) and ammonium ( $\text{NH}_4^+$ ) were  
210 collected in triplicate simultaneously to dissolved  $\text{N}_2:\text{Ar}$ , filtered through Whatman GF/F glass fiber  
211 filters, transferred to polyethylene vials and frozen for later analysis.  $\text{NH}_4^+$  was determined on a  
212 double beam Jasco V-550 spectrophotometer using salicylate and hypochlorite in the presence of  
213 sodium nitroprusside (Bower and Holm-Hansen, 1980).  $\text{NO}_2^-$  and  $\text{NO}_3^-$  were measured on a  
214 Technicon AutoAnalyser II (Armstrong et al., 1967). Detection limits were  $0.5 \mu\text{M}$ ,  $0.1 \mu\text{M}$ , and  $0.4$   
215  $\mu\text{M}$  for  $\text{NH}_4^+$ ,  $\text{NO}_2^-$ , and  $\text{NO}_3^-$ , respectively. Precision ranged between  $\pm 3\%$  and  $\pm 5\%$  for the three

216 nutrient analyses. DIN mass balance ( $\text{mol N h}^{-1}$ ) was determined as the difference in DIN load  
217 (calculated multiplying concentrations by water flow) between upstream and downstream sampling  
218 stations. Uncertainty in reach-scale mass balances was estimated by considering the variability in  
219 replicates for  $\text{NH}_4^+$ ,  $\text{NO}_2^-$ , and  $\text{NO}_3^-$  determination and the potential errors in flow measurements  
220 (Bukaveckas and Isenberg, 2013). Net DIN loss along each selected ditch was divided by the  
221 corresponding riverbed surface to obtain areal rates ( $\text{mmol N m}^{-2} \text{h}^{-1}$ ). Daily rates ( $\text{mmol N m}^{-2} \text{d}^{-1}$ )  
222 were calculated from hourly dark and light rates as described in section 2.2 for reach-scale  $\text{N}_2$  fluxes.  
223 Since  $\text{NO}_3^-$  was the dominant form of DIN ( $\text{NO}_3^-:\text{DIN} > 99\%$  in all samples), and  $\text{NH}_4^+$  and  $\text{NO}_2^-$   
224 concentration were close or below detection limits, hereafter we used the term  $\text{NO}_3^-$  removal instead  
225 of DIN removal.

226 At V, vegetation sampling was performed for the dominant species (*T. arundinacea*) according to  
227 Pierobon et al. (2013). Briefly, macrophyte % coverage (areal cover of the stream bed) and plant  
228 biomass were estimated in five replicates on each sampling date. Biomass was harvested with a 50x50  
229 cm frame randomly positioned and the dry weight (DW) measured after 36 h at 60°C. Average values  
230 of relative growth rates (RGR,  $\% \text{day}^{-1}$ ) representative of the three key stages of the plant growth  
231 cycle (spring, summer, and autumn) were calculated from biomass dry weight between two  
232 subsequent sampling campaigns. Uptake by in-stream vegetation was then obtained from the  
233 measured relative growth rates and areal coverages, and using an average N content in *T. arundinacea*  
234 biomass (Borin and Salvato, 2012). The biomass loss via herbivory was neglected due to the  
235 refractory nature of the macrophyte biomass.

#### 236 237 *2.4 Fluxes of $\text{O}_2$ , $\text{N}_2$ , and DIN and denitrification rates in sediment cores*

238 In May, twelve intact sediment cores (Plexiglas liners, i.d. 4.5 cm, height 20 cm) were collected  
239 manually from each ditch, eight for measurements of benthic fluxes and four for sediment  
240 characterization. At V, the sediments were sampled within the *T. arundinacea* stands but avoiding

241 the inclusion of plants into the cores. Sampling, pre-incubation and incubation procedures were  
242 performed according to a standard protocol (Dalsgaard et al., 2000). Briefly, once in the laboratory,  
243 eight cores from each ditch were submersed into incubation tanks with *in situ* water and left overnight.  
244 Homogeneous mixing of the water column without sediment resuspension was ensured by a rotating  
245 teflon-coated magnetic bar fixed to the inner wall of each liner a few centimetres above the sediment  
246 surface and driven by an external motor (40 rpm). Water was stirred during the whole pre-incubation  
247 and incubation periods. Dark gas (O<sub>2</sub>, N<sub>2</sub>) and dissolved inorganic N (NO<sub>3</sub><sup>-</sup>, NO<sub>2</sub><sup>-</sup>, NH<sub>4</sub><sup>+</sup>) exchange  
248 rates between water and sediment were measured by start-end batch incubations performed in ditch  
249 water at ~16°C, the average temperature typically maintained by the lowland springs water all year  
250 round (Laini et al., 2011). Incubation time (~2 h) was set in order to keep the variation of dissolved  
251 oxygen within ~20% of the initial value. The day after sampling, the water inside the cores was  
252 replaced with fresh ditch water and the incubations started when each liner was sealed with a floating  
253 Plexiglas lid. Oxygen was measured with a microsensor (OX-500, Unisense, Science Park Aarhus,  
254 Denmark) directly inside the cores at the beginning and end of the incubation, and simultaneously,  
255 water samples were collected from each core with a glass 100-mL syringe. Water samples for N<sub>2</sub>:Ar  
256 ratio and DIN measurements were collected and analyzed as previously described. Hourly dark fluxes  
257 of O<sub>2</sub>, N<sub>2</sub>, NH<sub>4</sub><sup>+</sup>, NO<sub>3</sub><sup>-</sup> and NO<sub>2</sub><sup>-</sup> were calculated from the rate of change in concentrations with time  
258 and expressed as rate per square meter, according to the equation:

259 
$$F = \frac{(C_f - C_0) \cdot V}{A \cdot t},$$

260 where F (μmol m<sup>-2</sup> h<sup>-1</sup>) is the flux, C<sub>0</sub> and C<sub>f</sub> (μM) are the concentrations at the beginning and at the  
261 end of incubation, respectively, V (L) is the water volume in the core, A (m<sup>2</sup>) is the surface of the  
262 sediment core, and t (h) is the incubation time. Negative values indicate a flux from the water column  
263 to the sediment (net consumption), while positive values indicate a flux from the sediment to the  
264 water column (net release). Daily fluxes were calculated by multiplying hourly rates by 24, since in

265 groundwater feeding lowland springs chlorophyll-*a* concentration is very low and photosynthetic  
266 activity considered irrelevant.

267 On the same set of cores used for benthic flux determinations, dark denitrification rates were  
268 measured by the isotope pairing technique (IPT, Nielsen, 1992; Dalsgaard et al., 2000), which allows  
269 for partitioning the total denitrification rates ( $D_{\text{tot}}$ ) into denitrification of  $\text{NO}_3^-$  diffusing to the anoxic  
270 sediment from the water column ( $D_{\text{W}}$ ), and denitrification of  $\text{NO}_3^-$  produced by nitrification within  
271 the oxic sediment ( $D_{\text{N}}$ ). At the beginning of the incubation, labelled  $\text{NO}_3^-$  (15 mM  $\text{Na}^{15}\text{NO}_3$  solution,  
272 98 atom% enrichment) was added to the water column of each core to have a final  $^{15}\text{N}$  atom%  
273 enrichment of ~30%. The  $\text{NO}_3^-$  concentration was measured prior and after the addition of  $^{15}\text{NO}_3^-$  at  
274 the time the cores were closed in order to calculate the  $^{14}\text{N}:^{15}\text{N}$  ratio in the  $\text{NO}_3^-$  pool. Cores were  
275 incubated in dark conditions as previously described for benthic flux measurements. At the end of  
276 incubation, the whole sediment and water phases of each core were gently mixed and an aliquot of  
277 the slurry was transferred into 12-mL glass-tight vials and preserved by adding 200  $\mu\text{L}$  of  $\text{ZnCl}_2$   
278 saturated solution. The IPT samples were analysed for  $^{29}\text{N}_2$  and  $^{30}\text{N}_2$  by MIMS (Lunstrum and Aoki,  
279 2016). Denitrification rates were calculated according to the equations and assumptions of Nielsen  
280 (1992).

281 Finally, the top 0-1 cm sediment layer of four cores from each ditch was analysed for bulk density  
282 (measured as the weight of a known volume of fresh material) and porosity after oven drying at 70  
283 °C. Organic matter content (OM, %) was quantified as loss on ignition (LOI) in a muffle furnace at  
284 350°C for 3 hours on dry powdered sediment aliquots.

285

## 286 *2.5 Statistical analyses*

287 The effect of factors *site* (V, U), *months* (May, July, September), and *light condition* (light, dark) on  
288 reach-scale net  $\text{N}_2$  fluxes was tested by means of a three-way ANOVA. Differences between the two  
289 ditches in  $\text{N}_2$  concentrations, core benthic fluxes and sediment features were tested via one-way

290 ANOVA. Normality (Shapiro–Wilk test) and homoscedasticity (Levene’s test) were previously  
291 examined. Log-transformed data satisfied assumptions of normality. Statistical significance was set  
292 at  $p \leq 0.05$ . Statistical analyses were performed with SigmaPlot 11.0 (Systat Software, Inc., CA, USA).

293

### 294 **3. Results**

#### 295 *3.1 General features of the investigated reaches*

296 Morphometric characteristics and water and sediment features of the two investigated ditches are  
297 reported in Table 1. Discharge showed a wide variation in the study period in both ditches, ranging  
298 from 10 to  $>140 \text{ L s}^{-1}$ , with the lower values detected in July since water flow from the spring  
299 decreased due to management for crop irrigation. At V, this period overlapped with the macrophyte  
300 coverage peak and the lowest values of water velocity.  $k_{600}$  values predicted as a function of current  
301 velocity and water depth were in the range 1.2-4.6 and 0.91-6.38  $\text{cm h}^{-1}$ , at V and U, respectively.  
302 Chemico-physical features of the inflowing water reflected the typical quality of emerging  
303 groundwater feeding the canal network in the study area. Temperature remained almost constant  
304 throughout the study period (15-17°C), oxygen was generally undersaturated (74-94%), conductivity  
305 was always higher than  $566 \mu\text{S cm}^{-1}$ , and  $\text{NO}_3^-$  concentrations were stably high and in the range 355-  
306 395  $\mu\text{M}$  (Table 1). Dissolved  $\text{N}_2$  concentrations at upstream sampling stations were in the range of  
307 573-612  $\mu\text{M}$  and not significantly different between V and U ( $p > 0.05$ ), but were significantly higher  
308 than theoretical water-atmosphere equilibrium concentrations ( $p < 0.01$ ) which correspond to a  
309 constant oversaturation in the range 101-105% (Table 1).

310

#### 311 *3.2 Reach-scale fluxes of $\text{N}_2$ and $\text{NO}_3^-$ and N uptake by vegetation*

312  $\text{N}_2$  concentrations measured at downstream sampling stations always exceeded concentrations  
313 predicted by de-gassing with the atmosphere and the excess was ascribed to in-stream  $\text{N}_2$  production.  
314 The only exception was measured at U, in May, in light conditions, when a null  $\text{N}_2$  production was

315 obtained.  $N_2$  production was significant different between ditches ( $p < 0.01$ ) varying in the ranges 1.2-  
316 5.5 and 0-2.1  $\text{mmol N m}^{-2} \text{h}^{-1}$  in presence (V) and absence (U) of vegetation, respectively (Fig. 2).  $N_2$   
317 fluxes were systematically higher in dark than in light conditions ( $p < 0.01$ ) at V and varied among  
318 seasons ( $p < 0.01$ ), with the highest  $N_2$  production rates measured in July for both ditches. No  
319 significant interactions among the three factors were found.

320 Despite the constancy of  $\text{NO}_3^-$  concentrations ( $\text{NO}_3^-:\text{DIN}$  always  $>99\%$ ), inflow  $\text{NO}_3^-$  loads varied  
321 between 13 and  $\sim 201 \text{ mol N h}^{-1}$ , according to discharges variation of the two ditches throughout the  
322 study period (Table 2), with the lower loads detected in July at V and the highest ones in September  
323 at U. In all sampling conditions,  $\text{NO}_3^-$  load measured downstream was lower than upstream in the  
324 range 0.3-20%. The highest  $\text{NO}_3^-$  removal rates expressed on an areal basis ( $2.5 \text{ mmol N m}^{-2} \text{h}^{-1}$ ) were  
325 detected at V in July (dark condition) when discharge was the lowest and retention times the highest,  
326 while the lowest one ( $0.4 \text{ mmol N m}^{-2} \text{h}^{-1}$ ) was measured at U in September (dark condition) (Fig. 2).  
327 Throughout the study period,  $\text{NO}_3^-$  abatement ranged between 0.5 and  $2.5 \text{ mmol N m}^{-2} \text{h}^{-1}$  in the  
328 vegetated ditch and between 0.4 and  $1.6 \text{ mmol N m}^{-2} \text{h}^{-1}$  in the unvegetated one (Fig. 2).  $N_2$  production  
329 rates were positively correlated with  $\text{NO}_3^-$  removal rates ( $r=0.77$ ,  $p < 0.01$ ,  $n=12$ ). For each sampling  
330 date, the highest rates ( $N_2$  production or  $\text{NO}_3^-$  consumption) were measured in the vegetated ditch  
331 during the dark phase.

332 The portion of ditch bed covered by *T. arundinacea* stands was 15%, 56%, and 42% in May, July and  
333 September respectively, with minimum average biomass in spring ( $100\text{-}300 \text{ gDW m}^{-2}$ ) and maximum  
334 values in autumn ( $550\text{-}650 \text{ gDW m}^{-2}$ ). The maximum values of RGR were obtained in May ( $4.0\text{-}7.0$   
335  $\% \text{ day}^{-1}$ ), intermediate rates in July ( $2.0\text{-}3.5\% \text{ day}^{-1}$ ) and the minimum values in September ( $0.1\text{-}0.2$   
336  $\% \text{ d}^{-1}$ ), resulting in a net daily biomass accumulation of 8-14, 10-18, and 1-2  $\text{g DW m}^{-2} \text{day}^{-1}$  in the  
337 three seasonal sampling campaigns, respectively. N uptake was maximum in July ( $11\text{-}19 \text{ mmol N m}^{-2}$   
338  $\text{d}^{-1}$ ), intermediate in May ( $9\text{-}15 \text{ mmol N m}^{-2} \text{d}^{-1}$ ) and minimum in September ( $1\text{-}2 \text{ mmol N m}^{-2} \text{d}^{-1}$ ).

339  
340 *3.3 Fluxes of  $O_2$ ,  $N_2$ , and DIN and denitrification rates in sediment cores*

341 Benthic fluxes of gas ( $O_2$ ,  $N_2$ ) and inorganic N forms ( $NH_4^+$ ,  $NO_3^-$ ) and denitrification rates measured  
342 in sediment cores were significantly different between the two ditches ( $p < 0.01$ ). Sediment oxygen  
343 consumption was 2 times higher at V ( $2.66 \pm 0.49 \text{ mmol } O_2 \text{ m}^{-2} \text{ h}^{-1}$ ) than U ( $1.35 \pm 0.42 \text{ mmol } O_2 \text{ m}^{-2}$   
344  $\text{h}^{-1}$ ) (Fig. 3). Sediments from V had significantly higher ( $p < 0.05$ ) OM content and porosity and  
345 significantly lower ( $p < 0.05$ ) density than sediments from U (Table 1).  $NH_4^+$  was always released  
346 from the sediment to the water column, with a significantly higher flux at V ( $0.14 \pm 0.08 \text{ mmol N m}^{-2}$   
347  $\text{h}^{-1}$ ) than at U ( $< 0.01 \text{ mmol N m}^{-2} \text{ h}^{-1}$ ). Benthic compartment was a sink for  $NO_3^- + NO_2^-$  with  
348 consumption rates higher at V ( $-0.77 \pm 0.44 \text{ mmol N m}^{-2} \text{ h}^{-1}$ ) than at U ( $-0.22 \pm 0.07 \text{ mmol N m}^{-2} \text{ h}^{-1}$ ).  
349 They were consistent with net  $N_2$  fluxes which were on average more than 4 times higher at V  
350 ( $0.59 \pm 0.25 \text{ mmol N m}^{-2} \text{ h}^{-1}$ ) than at U ( $0.13 \pm 0.1 \text{ mmol N m}^{-2} \text{ h}^{-1}$ ).

351 Total denitrification rates ( $D_{tot}$ ) measured via IPT were  $0.48 \pm 0.13 \text{ mmol N m}^{-2} \text{ h}^{-1}$  at V and  $0.06 \pm 0.02$   
352  $\text{mmol N m}^{-2} \text{ h}^{-1}$  at U, and the fraction sustained by water column  $NO_3^-$  ( $D_w$ ) on average accounted  
353 for  $86 \pm 12\%$  of  $D_{tot}$  at U and for  $68 \pm 21\%$  at V (Fig. 3).

354

### 355 *3.4 Reach-scale vs core measurements*

356 Throughout the study period, at V reach-scale  $NO_3^-$  removal varied between 22 and  $50 \text{ mmol N m}^{-2}$   
357  $\text{d}^{-1}$  and was consistent with the correspondent  $N_2$  production rates ( $38\text{-}84 \text{ mmol N m}^{-2} \text{ d}^{-1}$ ) (Fig. 4).  
358 The maximum values detected for open-channel  $N_2$  flux and  $NO_3^-$  abatement at U corresponded to  
359 the lower extremes of the ranges measured at V. Net N daily accumulation in plant biomass accounted  
360 for 5-8% of the daily reach-scale  $NO_3^-$  removal in May, 12-21% in July and 1-4% in September.  
361 Reach-scale rates ( $N_2$  production and  $NO_3^-$  consumption) were systematically higher throughout the  
362 study period than those obtained in laboratory by incubations of sediment cores (Fig. 4) with the  
363 maximum discrepancy found in summer for both V and U. For both ditches, there was no significant  
364 difference ( $p > 0.05$ ) between rates of  $N_2$  production obtained by  $N_2:Ar$  measurement and  
365 denitrification rates determined via IPT (Fig. 3).

366

## 367 4. Discussion

### 368 4.1 Vegetation promotes denitrification in $\text{NO}_3^-$ -rich ditches

369 In the present study, both  $\text{NO}_3^-$  consumption (measured via reach-scale mass balance) and  
370 denitrification (measured via  $\text{N}_2$  open-channel method) were 1.2-3.0 and 1.5-3.3-fold higher in the  
371 vegetated ditch compared to the unvegetated one, respectively. Aquatic vegetation can contribute to  
372 decreased N loads through two main pathways: directly via assimilation and incorporation into  
373 biomass, and indirectly, via the stimulation of microbially-mediated processes among which  
374 denitrification is the most important. Assimilation is only a temporary sequestration since N may be  
375 buried or recycled back to the aquatic system via leaching and mineralization of plant litter, while  
376 denitrification is a permanent N-removal (Schaller et al., 2004; Soana et al., 2015). Compared to daily  
377  $\text{NO}_3^-$  removal, N assimilation by *T. arundinacea* stands was irrelevant in May and September, but  
378 not in July when plant coverage peaked and  $\text{NO}_3^-$  uptake from the water column could not be  
379 excluded. However, *T. arundinacea*, like other helophytes, has a well-developed root system and  
380 assimilates N preferentially from the sediments in the form of  $\text{NH}_4^+$  (Brix et al., 1994).

381 Rooted macrophytes promote a number of “hidden dynamics”, both in the sediment around roots and  
382 in the periphytic mats, where N processing (e.g. uptake, ammonification, nitrification and  
383 denitrification) occurs with rates higher than those ascribed to the sediment alone (Schaller et al.,  
384 2004; Soana and Bartoli, 2014). The presence of vegetation stimulates the accumulation of organic  
385 matter (e.g. trapping suspended particles, root exudate release, decaying plant litter), thus providing  
386 to the benthic compartment both labile organic carbon availability and anoxic niches required for  
387  $\text{NO}_3^-$  dissimilation via denitrification (Li et al., 2016; Hang et al., 2016). Furthermore, submersed  
388 portions of plants, like stems and leaves, represent potentially available surfaces for hosting consortia  
389 of bacteria and microalgae. Biofilms can alter nutrient dynamics in shallow environments by being  
390 highly productive and promoting solute exchanges (Bastviken et al., 2003; Srivastava et al., 2016).  
391 Anyway, sediments without aquatic vegetation support denitrification too, even if with systematically  
392 lower rates. Anaerobic microsites around particulate organic matter and woody debris represent



393 suitable environments capable of promoting  $\text{NO}_3^-$  reduction by denitrifying bacteria (Schaller et al.,  
394 2004; Stelzer et al., 2014).

395 For the vegetated ditch, reach-scale  $\text{N}_2$  production and  $\text{NO}_3^-$  removal were systematically higher  
396 during dark conditions on each sampling occasion. Diurnal patterns of denitrification generally  
397 depend on oxygen dynamics resulting from a balance between photosynthesis and respiration  
398 processes (Laursen and Seitzinger, 2004; Pellerin et al., 2009; Lupon et al., 2016). Plant or benthic  
399 microalgal photosynthesis increases oxygen penetration, dislocating the denitrification zone deeper  
400 from the sediment-water interface and reducing the diffusional rate of  $\text{NO}_3^-$  towards the oxic–anoxic  
401 boundary where denitrification occurs. Conversely, in dark conditions, the oxic layer is thinner, the  
402 mean diffusional path length is shorter, thus the supply of  $\text{NO}_3^-$  from the water column to the  
403 denitrification zone is higher (Harrison et al., 2005; Nizzoli et al., 2014).

404 The general good agreement between reach-scale estimates of denitrification and  $\text{NO}_3^-$  consumption  
405 suggests that denitrification of water column  $\text{NO}_3^-$  was the main process responsible for N removal  
406 throughout the study period. Taking into account the associated variability by using a set of depth–  
407 velocity equations providing a range of  $k_{600}$  values,  $\text{N}_2$  production overlap  $\text{NO}_3^-$  removal in most  
408 cases. Indeed,  $\text{N}_2$  flux determinations suffer of the variability introduced by this conservative  
409 approach, failing direct measurements of the reaeration coefficients. However, when  $\text{N}_2$  fluxes were  
410 on average greater than the corresponding  $\text{NO}_3^-$  fluxes, we can postulate two hypothesis: 1)  
411 overestimation of  $\text{N}_2$  fluxes due to overestimation of the gas transfer velocity; 2) contribution of  
412 nitrification in producing  $\text{NO}_3^-$  subsequently denitrified to  $\text{N}_2$ . Determination of water-atmosphere  
413 gas exchanges is usually a critical step in open-channel methods. The use of empirical relationships  
414 for the calculation of gas transfer velocity carries a degree of uncertainty affecting the overall  
415 estimation of metabolic rates. Extensive literature reviews have highlighted that mathematical  
416 formulas including only the hydraulic parameters of water velocity and depth generally tend to predict  
417 higher  $k_{600}$  values than the real ones, except for the datasets used to calibrate them (Cox et al., 2003).  
418 As their performance is often uneven and contradictory, we cannot exclude that an overestimation of

419 reach-scale denitrification rates occurred for our investigated sites. Given that the identification of  
420 the appropriate equation for each specific velocity-depth range is usually difficult, future applications  
421 of the N<sub>2</sub> open-channel method should include the concomitant direct measurement of reaeration  
422 coefficients in order to increase the accuracy of the denitrification estimates. Denitrification rates  
423 measured by IPT in intact sediment cores demonstrated that the process was mostly supported by the  
424 reduction of NO<sub>3</sub><sup>-</sup> diffusing from the water column to anoxic sediments, but also nitrification in the  
425 oxic layers was a source of NO<sub>3</sub><sup>-</sup> for denitrification. This microbial path can be amplified in sediments  
426 hosting living roots where the injection of oxygen, generally conspicuous for emergent wetland  
427 plants, stimulates coupled nitrification/denitrification deeper in the rhizosphere (Borin and Salvato,  
428 2012; Taylor et al., 2015). However, in NH<sub>4</sub><sup>+</sup>-poor sites like ours, this pathway is likely to be of only  
429 minor influence on the measured reach-scale N<sub>2</sub> fluxes.

430

#### 431 *4.2 Main drivers of N removal*

432 Both proximal (biotic) and ecosystem-level (hydrologic) controls (Bernot and Dodds, 2005;  
433 Seitzinger et al., 2006) regulated temporal variability of denitrification rates in the studied ditches.  
434 On a daily basis, N-removal efficiency via denitrification was higher at night, likely due to anoxic  
435 zones closer to the supply of NO<sub>3</sub><sup>-</sup> from the water column. Otherwise, along the investigated period,  
436 flow rate was the most variable parameter exerting a primary control on in-stream N dynamics and  
437 denitrification. The highest rates of NO<sub>3</sub><sup>-</sup> removal and N<sub>2</sub> production were detected in July, when  
438 discharges were the lowest and retention times the highest. In fact, when the hydraulic residence time  
439 is long, ditches and canals function as linear wetlands, where interactions between water volumes and  
440 multiple biologically active interfaces are maximised, promoting N removal (Pinay et al., 2015;  
441 Tournebize et al., 2017).

442 The N removal rates (1.8-3.3 kg N km<sup>-1</sup>d<sup>-1</sup>) measured in this study in the vegetated ditch overlap those  
443 (1.5-5 kg N km<sup>-1</sup>d<sup>-1</sup>) previously measured with comparable methods in other vegetated ditches of the  
444 Po River hydrological network, used primarily for drainage and characterised by lower NO<sub>3</sub><sup>-</sup>

445 concentrations (30-150  $\mu\text{M}$ ) (Pierobon et al., 2013; Castaldelli et al., 2015). In the present study, the  
446 ditches were fed by  $\text{NO}_3^-$ -rich groundwater with concentrations up to 390  $\mu\text{M}$  almost constant during  
447 the year. Thus, similar denitrification rates, measured in ditches with 2.5-fold higher  $\text{NO}_3^-$   
448 concentrations, may indicate either a saturation of the process or a limitation by other regulating  
449 factors (Bernot and Dodds, 2005, Mulholland et al., 2008). Temperature stably close to 15-17°C may  
450 have limited denitrification. In fact, in ditches studied by Castaldelli et al. (2015), not fed by springs  
451 and located near the Po delta, summer water temperature was up to 29 °C. Furthermore,  
452 denitrification, being an anaerobic respiration, is controlled by the presence of an electron donor, in  
453 most of the cases represented by labile organic carbon. In the studied ditches, biodegradable carbon  
454 was not phytoplanktonic, since phytoplankton was almost absent (chlorophyll-*a* <0.5  $\mu\text{g L}^{-1}$ ), but  
455 more likely was produced in form of root exudates or from other plant decaying materials.  
456 Concentrations of dissolved organic carbon < 2  $\text{mg L}^{-1}$  were measured in the spring water feeding the  
457 studied ditches (Balestrini et al., 2016), indicating that organic carbon was unbalanced with respect  
458 to the large  $\text{NO}_3^-$  availability (4.9-5.5  $\text{mg N L}^{-1}$  on average, along the investigated period), according  
459 to the theoretical ratio of 1.07 of denitrification stoichiometry (Picek et al., 2007). Moreover, we can  
460 speculate that, not only the amount of organic carbon but probably also its biodegradability could  
461 have further limited denitrification. OM derived from emergent plants and woody riparian strips is  
462 generally refractory and undergoes slow decomposition, while exudates from the roots of aquatic  
463 vegetation are more easily degradable and may fuel microbial metabolism (Karjalainen et al., 2001;  
464 Hang et al., 2016).

465 It is reported that conditions of OM limitation may also favour incomplete denitrification and  $\text{N}_2\text{O}$   
466 production (Vilain et al., 2012; Zhao et al., 2014). This aspect was investigated in 15 ditches and  
467 canals, fed by spring water in the same geographical area, in early and late summer. Groundwater  
468 exhibited supersaturation of  $\text{N}_2\text{O}$  at the spring outlet, but in this specific case, no reach-scale  $\text{N}_2\text{O}$   
469 production was evidenced (Laini et al., 2011). These outcomes suggest that  $\text{N}_2\text{O}$  concentrations in  
470 ditches are regulated by outgassing of spring water affected by groundwater dynamics, while the

471 contribution of in-stream microbial or plant activity appears to be negligible with respect to the  
472 emissions of this greenhouse gas.

473

#### 474 *4.3 Management practices of the ditch network aimed at maximizing the depuration capacity*

475 The actual efficiency of small lotic ecosystems, such as ditches and canals, to mitigate N pollution  
476 can be really appreciated if they are considered as a whole, i.e. sediment, vegetation, biofilms and  
477 their multiple interactions. Reach-scale methods, that integrate water column and benthic  
478 compartments, allow the quantification of processes and dynamics not detectable through the  
479 laboratory incubations of sediment cores (Gardner et al., 2016; Reisinger et al., 2016). Therefore,  
480 they are more suitable for a better understanding of large-scale N processing with potential  
481 implications for management strategies of aquatic ecosystems in human-impacted catchments. Our  
482 results suggested that small size watercourses in agricultural landscapes are important hot spots of N  
483 removal especially in presence of vegetation. Even though high denitrification rates supported by  
484 agricultural ditches,  $\text{NO}_3^-$  loads transported by spring-fed waterways in the Lombardy Plain are very  
485 elevated (Laini et al., 2011; Sacchi et al., 2013), thus the in-stream  $\text{NO}_3^-$  removal measured in this  
486 study was actually relatively low. Downstream  $\text{NO}_3^-$  loads were generally lower than upstream ones  
487 by 0.2-3.9%, while during period of low discharge and maximum vegetation development, the  
488 percentage of in-stream reduction peaked at ~20%. These outcomes evidence one of the most valuable  
489 ecosystem services provided by aquatic vegetation, i.e. the mitigation of  $\text{NO}_3^-$  pollution, and sustain  
490 the need of increasing macrophytes biomass to favour denitrification. In routine management  
491 practices aimed at preserving the hydraulic performance of canals and ditches, aquatic vegetation is  
492 considered only as an impediment for water circulation and usually removed, sometimes together  
493 with sediments. A sustainable ditch maintenance able to harmonize the hydraulic functionality with  
494 some ecological issues is reliable and relatively costless. For example, the frequency and the  
495 extensions of the vegetation cutting can be regulated avoiding the complete and simultaneous removal  
496 in many ditches, while opting for spatially and temporally differentiated models of maintenance.

497 Also, a hydrological management of the ditch network able to maintain an appropriate water head,  
498 that means leaving enough water in the irrigation period and reducing the inflows during abundant  
499 rainy events, can support the removal of  $\text{NO}_3^-$ . An increase of the water residence time, a crucial  
500 factor for N retention, could be achieved by actions addressed at increasing the channel sinuosity and  
501 diversifying the flows, e.g. by inserting coarse substrates and large woody debris in the bed or by  
502 creating lentic units. On the other hand, hardwood riparian strips could act as a buffer for  $\text{NO}_3^-$  coming  
503 from the cultivated field through the subsurface flow paths. In the light of these outcomes, it is evident  
504 that a sustainable management of the agricultural catchments able to exploit the several ecosystems  
505 services provided by the natural systems (e.g. macrophytes and riparian zones) could contribute to  
506 counteract one of most widespread, costly and challenging environmental problems, i.e.  $\text{NO}_3^-$   
507 pollution.

508

## 509 **5. Conclusions**

510 The results from the present study show that: 1) ditches with in-stream vegetation provide a  
511 significantly higher  $\text{NO}_3^-$  removal than unvegetated ones; 2) plant-mediated denitrification is the  
512 dominant N removal pathway; 3) a longer water residence and larger development of interfaces on  
513 aquatic vegetation promote N abatement; and 4) addition of labile organic carbon by in-stream  
514 macrophyte helps to overcome the OM limitation typical of ditches fed only by spring water. In the  
515 light of these evidences, the ditch management should turn to practices which, though guaranteeing  
516 the hydraulic efficiency, may at the same time favour the above cited processes, during the plant  
517 growth cycle. These actions may significantly enhance N remediation capacity and other ecosystem  
518 services supported by macrophytes in hydraulic networks fed by  $\text{NO}_3^-$ -rich spring-water, with positive  
519 effects at the watershed level and on the terminal water bodies as, in the case of the Po basin, the  
520 coastal lagoon of the delta and north-western Adriatic Sea.

521

522 **Acknowledgments**

523 This work was financially supported by Lombardy Region and National Research Council - CNR  
524 within the FILAGRO Project.

525

526 **References**

527 Armstrong, F.A.J., Sterus, C.R., Strickland, J.D.H., 1967. The measurement of upwelling and  
528 subsequent biological processes by means of the Technicon AutoAnalyzer and associated equipment.  
529 *Deep-Sea Res.* 14, 381–389.

530 Balestrini, R., Arese, C., Delconte, C., 2008. Lacustrine wetland in an agricultural catchment:  
531 Nitrogen removal and related biogeochemical processes. *Hydrol. Earth Syst. Sci.* 12 (2), 539–550.

532 Balestrini, R., Sacchi, E., Tidili, D., Delconte, C. A., Buffagni, A., 2016. Factors affecting agricultural  
533 nitrogen removal in riparian strips: examples from groundwater-dependent ecosystems of the Po  
534 Valley (Northern Italy). *Agric. Ecosyst. Environ.* 221, 132–144.

535 Bartoli, M., Racchetti, E., Delconte, C. A., Sacchi, E., Soana, E., Laini, A., Longhi, D., Viaroli, P.,  
536 2012. Nitrogen balance and fate in a heavily impacted watershed (Oglio River, Northern Italy): in  
537 quest of the missing sources and sinks. *Biogeosciences* 9(1), 361–373.

538 Bastviken, S.K., Eriksson, P.G., Martins, I., Neto, J.M., Leonardson, L., Tonderski, K., 2003.  
539 Potential nitrification and denitrification on different surfaces in a constructed treatment wetland. *J.*  
540 *Environ. Qual.* 32(6), 2414–2420.

541 Beaulieu, J.J., Golden, H.E., Knightes, C.D., Mayer, P.M., Kaushal, S.S., Pennino, M.J., Arango,  
542 C.P., Balz, D.A., Elonen, C.M., Fritz, K.M., Hill, B.H., 2015. Urban stream burial increases  
543 watershed-scale nitrate export. *PloS one* 10(7), e0132256.

544 Bernot, M.J., Dodds, W.K., 2005. Nitrogen retention, removal, and saturation in lotic  
545 ecosystems. *Ecosystems* 8(4), 442–453.

546 Birgand, F., Skaggs, R.W., Chescheir, G.M., Gilliam, J.W., 2007. Nitrogen removal in streams of  
547 agricultural catchments – a literature review. *Crit. Rev. Env. Sci. Tech.* 37, 487–499.

548 Borin, M., Salvato, M., 2012. Effects of five macrophytes on nitrogen remediation and mass balance  
549 in wetland mesocosms. *Ecol. Eng.* 46, 34–42.

550 Bower, C.E., Holm-Hansen, T., 1980. A salicylate-hypochlorite method for determining ammonia in  
551 seawater. *Can. J. Fish. Aquat. Sci.* 37(5), 794–798.

552 Brix, H., Lorenzen, B., Morris, J.T., Schierup, H.H., Sorrell, B.K., 1994. Effects of oxygen and nitrate  
553 on ammonium uptake kinetics and adenylate pools in *Phalaris arundinacea* L. and *Glyceria maxima*  
554 (Hartm.) Holmb. *Proc. R. Soc. Edinburgh. Section B. Biological Sciences* 102, 333–342.

555 Bukaveckas, P.A., Isenberg, W.N., 2013. Loading, transformation, and retention of nitrogen and  
556 phosphorus in the tidal freshwater James River (Virginia). *Estuar. Coasts* 36(6), 1219–1236.

557 Castaldelli, G., Soana, E., Racchetti, E., Pierobon, E., Mastrocicco, M., Tesini, E., Bartoli, M., Fano,  
558 E.A., 2013. Nitrogen budget in a lowland coastal area within the Po River Basin (Northern Italy):  
559 multiple evidences of equilibrium between sources and internal sinks. *Environ. Manag.* 52, 567–580.

560 Castaldelli, G., Soana, E., Racchetti, E., Vincenzi, F., Fano, E. A., Bartoli, M., 2015. Vegetated canals  
561 mitigate nitrogen surplus in agricultural watersheds. *Agric. Ecosyst. Environ.* 212, 253–262.

562 Cox, B. A., 2003. A review of dissolved oxygen modelling techniques for lowland rivers. *Sci. Total*  
563 *Environ.* 314, 303–334.

564 Dalsgaard, T., Nielsen, L.P., Brotas, V., Viaroli, P., Underwood, G.J.C., Nedwell, D.B., Sundbäck,  
565 K., Rysgaard, S., Miles, A., Bartoli, M., Dong, L., Thornton, D.C.O., Ottosen, L.D.M., Castaldelli,  
566 G., Risgaard-Petersen, N., 2000. Protocol Handbook for NICE-Nitrogen Cycling in Estuaries: A  
567 Project Under the EU Research Programme. Marine Science and Technology (MAST III). National  
568 Environmental Research Institute, Silkeborg, Denmark, 62 pp.

569 Dollinger, J., Dagès, C., Bailly, J. S., Lagacherie, P., Voltz, M., 2015. Managing ditches for  
570 agroecological engineering of landscape. A review. *Agron. Sustain. Dev.* 35(3), 999–1020.

571 Duncan, J.M., Groffman, P.M., Band, L.E., 2013. Towards closing the watershed nitrogen budget:  
572 Spatial and temporal scaling of denitrification. *J. Geophys. Res-Bioge.* 118(3), 1105–1119.

573 Gardner, J.R., Fisher, T.R., Jordan, T.E., Knee, K.L., 2016. Balancing watershed nitrogen budgets:  
574 accounting for biogenic gases in streams. *Biogeochemistry* 127, 231–253.

575 Groffman, P.M., Bain, D.J., Band, L.E., Belt, K.T., Brush, G.S., Grove, J. M., Pouyat, R.V.,  
576 Yesilonis, I.C., Zipperer, W. C., 2003. Down by the riverside: urban riparian ecology. *Front. Ecol.*  
577 *Environ.* 1(6), 315–321.

578 Haider, H., Ali, W., Haydar, S., 2013. Evaluation of various relationships of reaeration rate coefficient  
579 for modeling dissolved oxygen in a river with extreme flow variations in Pakistan. *Hydrol. Process.*  
580 27, 3949–3963.

581 Hang, Q., Wang, H., Chu, Z., Ye, B., Li, C., Hou, Z., 2016. Application of plant carbon source for  
582 denitrification by constructed wetland and bioreactor: review of recent development. *Environ. Sci.*  
583 *Pollut. R.* 23(9), 8260–8274.

584 Harrison, J.A., Matson, P.A., Fendorf, S.E., 2005. Effects of a diel oxygen cycle on nitrogen  
585 transformations and greenhouse gas emissions in a eutrophied subtropical stream. *Aquat. Sci.* 67(3),  
586 308–315.

587 Hefting, M.M., van den Heuvel, R.N., Verhoeven, J.T., 2013. Wetlands in agricultural landscapes for  
588 nitrogen attenuation and biodiversity enhancement: Opportunities and limitations. *Ecol. Eng.* 56, 5–  
589 13.

590 Iseyemi, O.O., Farris, J.L., Moore, M.T., Choi, S.E., 2016. Nutrient Mitigation Efficiency in  
591 Agricultural Drainage Ditches: An Influence of Landscape Management. *B. Environ. Contam. Tox.*  
592 96(6), 750–756.



593 Jähne, B, Munnich, K.O., Bosinger, R., Dutzi, A., Huber, W., Libner, P., 1987. On parameters  
594 influencing air–water exchange. *J. Geophys. Res.* 92, 1937–1949.

595 Kana, T.M., Darkangelo, C., Hunt, M.D., Oldham, J.B., Bennett, G.E., Cornwell, J.C., 1994.  
596 Membrane inlet mass spectrometer for rapid high-precision determination of N<sub>2</sub>, O<sub>2</sub>, and Ar in  
597 environmental water samples. *Anal. Chem.* 66(23), 4166-4170.

598 Karjalainen, H., Stefansdottir, G., Tuominen, L., Kairesalo, T., 2001. Do submersed plants enhance  
599 microbial activity in sediment? *Aquat. Bot.* 69, 1–13.

600 Laini, A., Bartoli, M., Castaldi, S., Viaroli, P., Capri, E., Trevisan, M., 2011. Greenhouse gases (CO<sub>2</sub>,  
601 CH<sub>4</sub> and N<sub>2</sub>O) in lowland springs within an agricultural impacted watershed (Po River Plain, northern  
602 Italy). *Chem. Ecol.* 27(2), 177–187.

603 Laursen, A.E., Seitzinger, S.P., 2002. Measurement of denitrification in rivers: an integrated, whole  
604 reach approach. *Hydrobiologia* 485, 67–81.

605 Laursen, A.E., Seitzinger, S.P., 2004. Diurnal patterns of denitrification, oxygen consumption and  
606 nitrous oxide production in rivers measured at the whole-reach scale. *Fresh. Biol.* 49, 1448–1458.

607 Li, F., Pan, Y., Xie, Y., Chen, X., Deng, Z., Li, X., Hou, Z., Tang, Y., 2016. Different roles of three  
608 emergent macrophytes in promoting sedimentation in Dongting Lake, China. *Aquat. Sci.* 78(1), 159–  
609 169.

610 Lunstrum, A., Aoki, L.R., 2016. Oxygen interference with membrane inlet mass spectrometry may  
611 overestimate denitrification rates calculated with the isotope pairing technique. *Limnol. Oceanogr-*  
612 *Meth.* 14, 425–431.

613 Lupon, A., Martí, E., Sabater, F., Bernal, S., 2016. Green light: gross primary production influences  
614 seasonal stream N export by controlling fine-scale N dynamics. *Ecology* 97(1), 133–144.

615 Marion, A., Nikora, V., Puijalón, S., Bouma, T., Koll, K., Ballio, F., Tait, S., Zaramella, M.,  
616 Sukhodolov, A., O’Hare, M., Wharton, G., Aberle, J., Tregnaghi, M., Davies, P., Nepf, H., Parker,

617 G., Statzner, B., 2014. Aquatic interfaces: a hydrodynamic and ecological perspective. *J. Hydraul.*  
618 *Res.* 52, 744–758.

619 Mulholland, P.J., Helton, A.M., Poole, G.C., Hall, R.O. Jr, Hamilton, S.K., Peterson, B.J., Tank, J.L.,  
620 Ashkenas, L.R., Cooper, L.W., Dahm, C.N., Dodds, W.K., Findlay, S.E.G., Gregory, S.V., Grimm,  
621 N.B., Johnson, S.L., Mcdowell, W.H., Meyer, J.L., Valett, H.M., Webster, J.R., Arango, C.P.,  
622 Beaulieu, J.J., Bernot, M.J., Burgin, A.J., Crenshaw, C.L., Johnson, L.T., Niederlehner, B.R.,  
623 O’Brien, J.M., Potter, J.D., Sheibley, R.W., Sobota, D.J., Thomas, S.M., 2008. Stream denitrification  
624 across biomes and its response to anthropogenic nitrate loading. *Nature* 452, 202–205.

625 Nielsen, L.P., 1992. Denitrification in sediment determined from nitrogen isotope pairing. *FEMS*  
626 *Microbiol. Lett.* 86(4), 357-362.

627 Nizzoli, D., Welsh, D.T., Longhi, D., Viaroli, P., 2014. Influence of *Potamogeton pectinatus* and  
628 microphytobenthos on benthic metabolism, nutrient fluxes and denitrification in a freshwater littoral  
629 sediment in an agricultural landscape: N assimilation versus N removal. *Hydrobiologia* 737, 183–  
630 200.

631 Pellerin, B. A., Downing, B. D., Kendall, C., Dahlgren, R. A., Kraus, T. E., Saraceno, J., Spencer,  
632 R.G.M., Bergamaschi, B. A., 2009. Assessing the sources and magnitude of diurnal nitrate variability  
633 in the San Joaquin River (California) with an in situ optical nitrate sensor and dual nitrate isotopes.  
634 *Fresh. Biol.* 54(2), 376–387.

635 Picek, T., Čížková, H., Dušek, J., 2007. Greenhouse gas emissions from a constructed wetland—  
636 plants as important sources of carbon. *Ecol. Eng.* 31(2), 98–106.

637 Pierce, S.C., Kröger, R., Pezeshki, R., 2012. Managing artificially drained low-gradient agricultural  
638 headwaters for enhanced ecosystem functions. *Biology* 1, 794–856.

639 Pierobon, E., Castaldelli, G., Mantovani, S., Vincenzi, F., Fano, E.A., 2013. Nitrogen removal in  
640 vegetated and unvegetated drainage ditches impacted by diffuse and point sources of pollution. *Clean*  
641 *Soil Air Water* 41, 24–31.

642 Pinay, G., Peiffer, S., De Dreuzy, J.R., Krause, S., Hannah, D.M., Fleckenstein, J.H., Sebiló, M.,  
643 Bishop, K., Hubert-Moy, L., 2015. Upscaling nitrogen removal capacity from local hotspots to low  
644 stream orders' drainage basins. *Ecosystems* 18, 1101–1120.

645 Racchetti, E., Longhi, D., Ribaudó, C., Soana, E., Bartoli, M. Nitrogen uptake and coupled  
646 nitrification–denitrification in riverine sediments with benthic microalgae and rooted macrophytes.  
647 *Aquatic Sciences*, in press.

648 Reisinger, A.J., Tank, J.L., Hoellein, T.J., Hall, R.O., 2016. Sediment, water column, and open-  
649 channel denitrification in rivers measured using membrane-inlet mass spectrometry. *Journal of*  
650 *Geophysical Research: Biogeosciences* 121(5), 1258-1274.

651 Roley, S.S., Tank, J.L., Stephen, M.L., Johnson, L.T., Beaulieu, J.J., Witter, J.D., 2012. Floodplain  
652 restoration enhances denitrification and reach-scale nitrogen removal in an agricultural stream. *Ecol.*  
653 *Appl.* 22(1), 281–297.

654 Romero, E., Garnier, J., Billen, G., Peters, F., Lassaletta, L., 2016. Water management practices  
655 exacerbate nitrogen retention in Mediterranean catchments. *Sci. Total Environ.* 573, 420–432.

656 Sacchi, E., Acutis, M., Bartoli, M., Brenna, S., Delconte, C. A., Laini, A., Pennisi, M., 2013. Origin  
657 and fate of nitrates in groundwater from the central Po plain: insights from isotopic  
658 investigations. *Appl. Geochem* 34, 164–180.

659 Schaller, J.L., Royer, T.V., David, M.B., Tank, J.L., 2004. Denitrification associated with plants and  
660 sediments in an agricultural stream. *J. N. Am. Benthol. Soc.* 23(4), 667–676.

661 Schwarzenbach R., Gschwend P.M., Imboden, D.M., 1993. *Environmental Organic Chemistry*,  
662 Wiley, NewYork.

663 Seitzinger, S., Harrison, J.A., Böhlke, J.K., Bouwman, A.F., Lowrance, R., Peterson, B., Tobias, C.,  
664 Drecht, G.V., 2006. Denitrification across landscapes and waterscapes: a synthesis. *Ecol. Appl.* 16(6),  
665 2064–2090.

666 Soana, E., Bartoli, M., 2014. Seasonal regulation of nitrification in a rooted macrophyte (*Vallisneria*  
667 *spiralis* L.) meadow under eutrophic conditions. *Aquat. Ecol.* 48(1), 11–21.

668 Soana, E., Naldi, M., Bonaglia, S., Racchetti, E., Castaldelli, G., Brüchert, V., Viaroli, P., Bartoli,  
669 M., 2015. Benthic nitrogen metabolism in a macrophyte meadow (*Vallisneria spiralis* L.) under  
670 increasing sedimentary organic matter loads. *Biogeochemistry* 124(1-3), 387–404.

671 Srivastava, J. K., Chandra, H., Kalra, S.J., Mishra, P., Khan, H., Yadav, P., 2016. Plant–microbe  
672 interaction in aquatic system and their role in the management of water quality: a review. *Appl. Water*  
673 *Sci.* 1–12.

674 Stelzer, R.S., Scott, J.T., Bartsch, L.A., Parr, T.B., 2014. Particulate organic matter quality influences  
675 nitrate retention and denitrification in stream sediments: evidence from a carbon burial experiment.  
676 *Biogeochemistry* 119(1-3), 387–402.

677 Taylor, J.M., Moore, M.T., Scott, J.T., 2015. Contrasting nutrient mitigation and denitrification  
678 potential of agricultural drainage environments with different emergent aquatic macrophytes. *J.*  
679 *Envir. Qual.* 44(4), 1304–1314.

680 Tournebize, J., Chaumont, C., Mander, Ü., 2017. Implications for constructed wetlands to mitigate  
681 nitrate and pesticide pollution in agricultural drained watersheds. *Ecol. Eng.* In press

682 Viaroli, P., Nizzoli, D., Pinardi, M., Soana, E., Bartoli, M., 2015. Eutrophication of the Mediterranean  
683 Sea: a watershed—cascading aquatic filter approach. *Rend. Lincei* 26(1), 13–23.

684 Vilain, G., Garnier, J., Tallec, G., Tournebize, J., 2012. Indirect N<sub>2</sub>O emissions from shallow  
685 groundwater in an agricultural catchment (Seine Basin, France). *Biogeochemistry*, 111(1-3), 253-  
686 271.

- 687 Wanninkhof, R., 1992. Relationship between gas exchange and wind speed over the ocean. J.  
688 Geophys. Res. 97, 7373–7381.
- 689 Weiss, R.F., 1970. The solubility of nitrogen, oxygen and argon in water and seawater. Deep-Sea  
690 Res. 17(4), 721-735.
- 691 Zhao, Y., Xia, Y., Li, B., Yan, X., 2014. Influence of environmental factors on net N<sub>2</sub> and N<sub>2</sub>O  
692 production in sediment of freshwater rivers. Environmental Science and Pollution Research, 21(16),  
693 9973-9982.

694 **Table 1.** Morphometric characteristics and water and sediment features of the two investigated  
 695 ditches. Discharge, velocity and transit time are reported as average  $\pm$  standard deviation of three  
 696 cross sections along each ditch. Depths are measured in the central portion of each ditch. Gas transfer  
 697 velocity (k600) is calculated as described in section 2.2. Water physical and chemical parameters,  
 698 measured at the upstream station, are average values  $\pm$  standard deviation of the dark and light  
 699 samplings in each period. Sediment features were measured on 4 cores sampled in each ditch.

|                                   |                               | V                                   | U            |
|-----------------------------------|-------------------------------|-------------------------------------|--------------|
|                                   |                               | Length (m)                          | 380          |
|                                   |                               | Width (m)                           | 2.8          |
|                                   |                               | k600 (cm h <sup>-1</sup> )          | 1.2-4.6      |
| Morphometric parameters           | May                           | Discharge (L s <sup>-1</sup> )      | 40 (8)       |
|                                   |                               | Velocity (cm s <sup>-1</sup> )      | 6 (1)        |
|                                   |                               | Depth (cm)                          | 30-40        |
|                                   |                               | Transit time (min)                  | 115 (23)     |
|                                   | July                          | Discharge (L s <sup>-1</sup> )      | 10 (2)       |
|                                   |                               | Velocity (cm s <sup>-1</sup> )      | 2 (1)        |
|                                   |                               | Depth (cm)                          | 10-20        |
|                                   |                               | Transit time (min)                  | 270 (55)     |
|                                   | September                     | Discharge (L s <sup>-1</sup> )      | 106 (23)     |
|                                   |                               | Velocity (cm s <sup>-1</sup> )      | 10 (2)       |
|                                   |                               | Depth (cm)                          | 40-50        |
|                                   |                               | Transit time (min)                  | 72 (16)      |
| Chemical - physical parameters    | May                           | T (°C)                              | 15.62 (0.75) |
|                                   |                               | Conductivity (μS cm <sup>-1</sup> ) | 665 (6)      |
|                                   |                               | O <sub>2</sub> saturation (%)       | 84 (14)      |
|                                   |                               | NO <sub>3</sub> <sup>-</sup> (μM)   | 395 (2)      |
|                                   |                               | N <sub>2</sub> (μM)                 | 593 (18)     |
|                                   |                               | N <sub>2</sub> saturation (%)       | 103 (2)      |
|                                   | July                          | T (°C)                              | 16.37 (0.48) |
|                                   |                               | Conductivity (μS cm <sup>-1</sup> ) | 634 (11)     |
|                                   |                               | O <sub>2</sub> saturation (%)       | 77 (26)      |
|                                   |                               | NO <sub>3</sub> <sup>-</sup> (μM)   | 355 (6)      |
|                                   |                               | N <sub>2</sub> (μM)                 | 586 (16)     |
|                                   |                               | N <sub>2</sub> saturation (%)       | 103 (2)      |
|                                   | September                     | T (°C)                              | 16.58 (0.93) |
|                                   |                               | Conductivity (μS cm <sup>-1</sup> ) | 621 (4)      |
|                                   |                               | O <sub>2</sub> saturation (%)       | 94 (33)      |
| NO <sub>3</sub> <sup>-</sup> (μM) |                               | 389 (6)                             |              |
| N <sub>2</sub> (μM)               |                               | 573 (15)                            |              |
| N <sub>2</sub> saturation (%)     |                               | 101 (1)                             |              |
| Sediment features                 | Density (g mL <sup>-1</sup> ) | 1.46 (0.16)                         |              |
|                                   | Porosity                      | 0.66 (0.09)                         |              |
|                                   | Organic matter (%)            | 4.22 (1.67)                         |              |

701 **Table 2.** Upstream hourly NO<sub>3</sub><sup>-</sup> loads (average ± standard deviation) and average percentages of NO<sub>3</sub><sup>-</sup>  
702 removal ( $\Delta < 0$ ) in light and dark conditions;  $\Delta$  is calculated as (downstream load – upstream  
703 load)/upstream load x 100. The percentage of NO<sub>3</sub><sup>-</sup> with respect to DIN (dissolved inorganic nitrogen)  
704 is also reported.  
705

|           |  | V           |              | U           |              |
|-----------|--|-------------|--------------|-------------|--------------|
|           |  | <i>Dark</i> | <i>Light</i> | <i>Dark</i> | <i>Light</i> |
| May       | <b>Upstream NO<sub>3</sub><sup>-</sup> load</b> (mol N h <sup>-1</sup> ) | 157 (12)    | 156 (34)     | 91 (17)     | 92 (16)      |
|           | <b><math>\Delta</math> load</b>  | -3.90%      | -0.37%       | -1.96%      | -0.28%       |
|           | <b>NO<sub>3</sub><sup>-</sup>:DIN</b>                                    | 99.89%      | 99.70%       | 99.95%      | 99.28%       |
| July      | <b>Upstream NO<sub>3</sub><sup>-</sup> load</b> (mol N h <sup>-1</sup> ) | 13 (2)      | 13 (2)       | 19 (6)      | 20 (6)       |
|           | <b><math>\Delta</math> load</b>  | -20.89%     | -16.33%      | -3.82%      | -3.81%       |
|           | <b>NO<sub>3</sub><sup>-</sup>:DIN</b>                                    | 99.57%      | 99.50%       | 99.92%      | 99.94%       |
| September | <b>Upstream NO<sub>3</sub><sup>-</sup> load</b> (mol N h <sup>-1</sup> ) | 146 (32)    | 150 (34)     | 197 (7)     | 201 (7)      |
|           | <b><math>\Delta</math> load</b>  | -1.50%      | -0.61%       | -0.23%      | -0.29%       |
|           | <b>NO<sub>3</sub><sup>-</sup>:DIN</b>                                    | 99.75%      | 99.92%       | 99.91%      | 99.96%       |

706

707 **Figure captions**

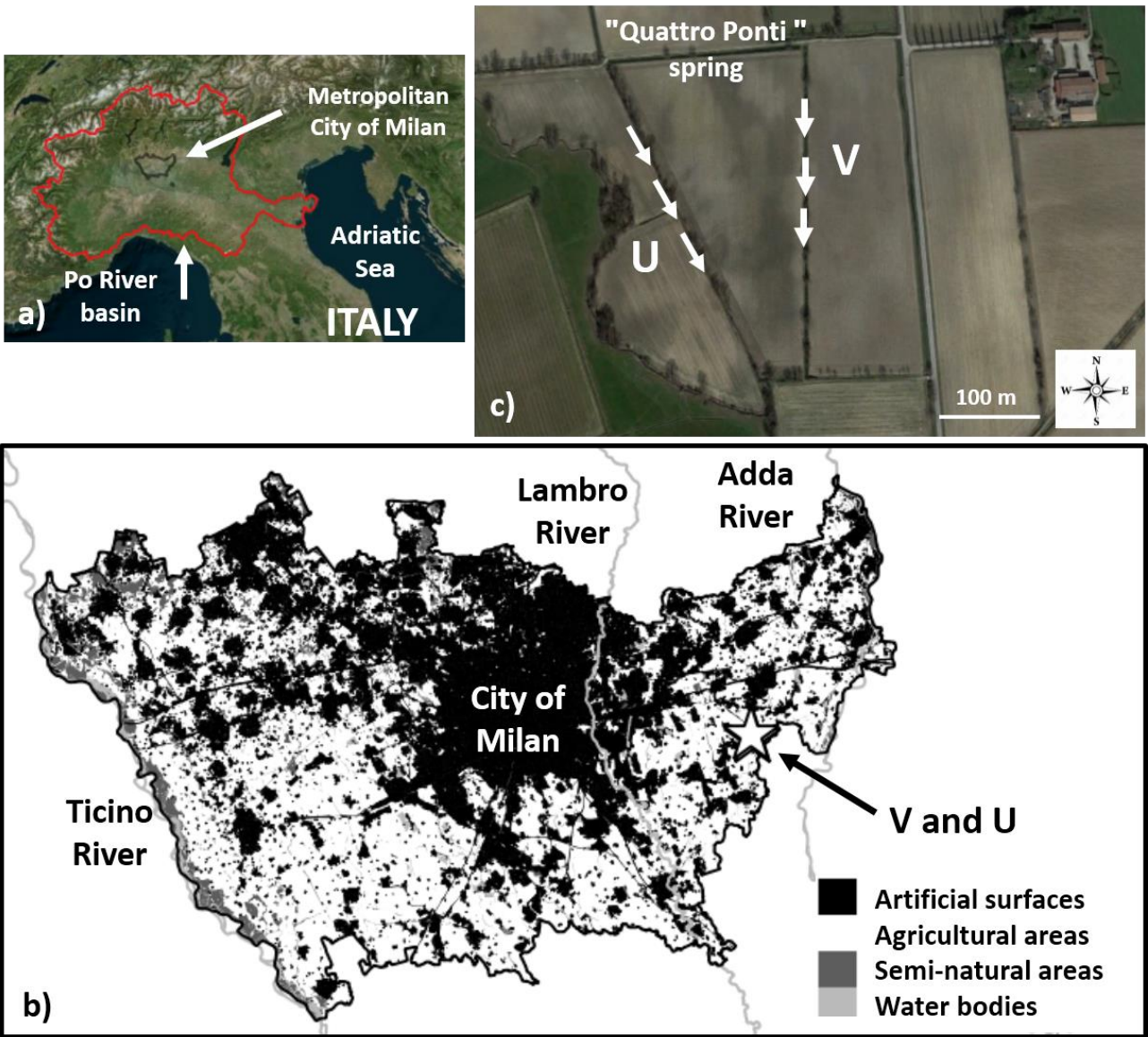
708 **Figure 1.** Location of the two investigated ditches: a) the Po River basin and the Metropolitan City  
709 of Milan (Northern Italy); b) the land use of the Metropolitan City of Milan (DUSAF cartographic  
710 database - Land Use of Agricultural and Forest Land, Lombardy Region, 2012); c) the spring “Quattro  
711 Ponti” and the two ditches (V and U), with the flow path indicated. Geographic data showed in the  
712 maps were downloaded from the Lombardy Region Geoportal  
713 (<http://www.geoportale.regione.lombardia.it/>).

714 **Fig. 2.** Hourly rates of  $\text{NO}_3^-$  removal (box below) and  $\text{N}_2$  production (box at the top) measured in the  
715 two investigated ditches throughout the study period (average $\pm$ standard deviation). Rates obtained at  
716 the reach-scale in light and dark conditions are compared. In May at U,  $\text{N}_2$  production was null for  
717 light sampling.

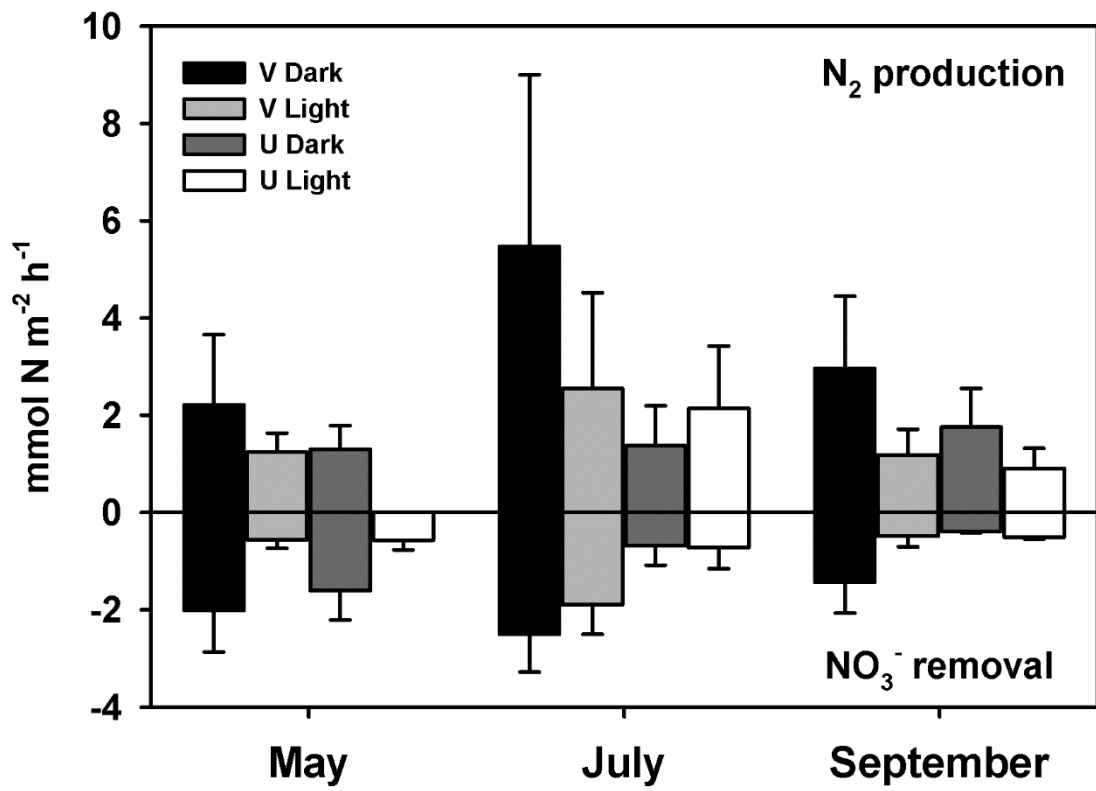
718 **Fig. 3.** Benthic fluxes of  $\text{O}_2$ ,  $\text{NH}_4^+$ ,  $\text{NO}_3^-$ ,  $\text{N}_2$ , and denitrification rates measured via incubations of  
719 sediment cores sampled in the two ditches (average $\pm$ standard deviation).  $\text{NO}_3^-$  fluxes include also  
720  $\text{NO}_2^-$  contribution never exceeding 2%. Denitrification rates determined by IPT (isotope pairing  
721 technique) are split in the contribution of Dw (denitrification of water column  $\text{NO}_3^-$ ) and Dn  
722 (denitrification of  $\text{NO}_3^-$  produced by nitrification in the oxic sediment layer).

723 **Fig. 4.** Daily rates of  $\text{NO}_3^-$  removal (box below) and  $\text{N}_2$  production (box at the top) measured in the  
724 two investigated ditches throughout the study period (average $\pm$ standard deviation). Rates obtained at  
725 the reach-scale (in May, July, and September) and by core incubations (in May) are compared.



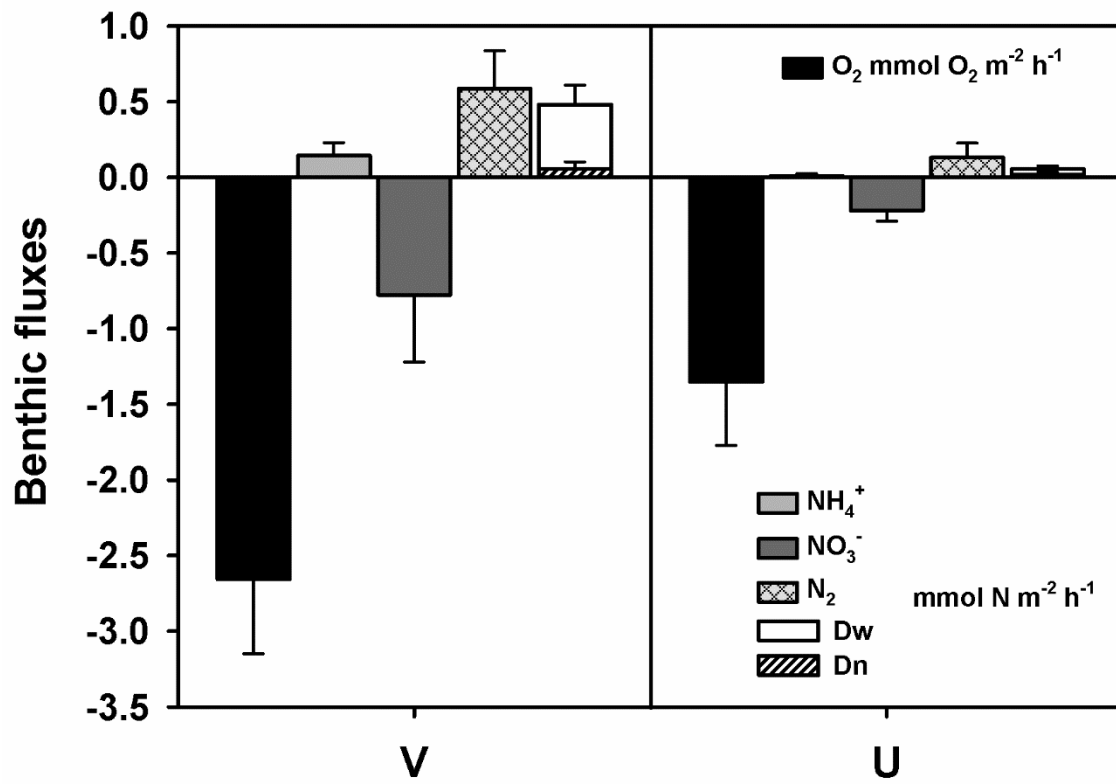


726  
727 Fig. 1

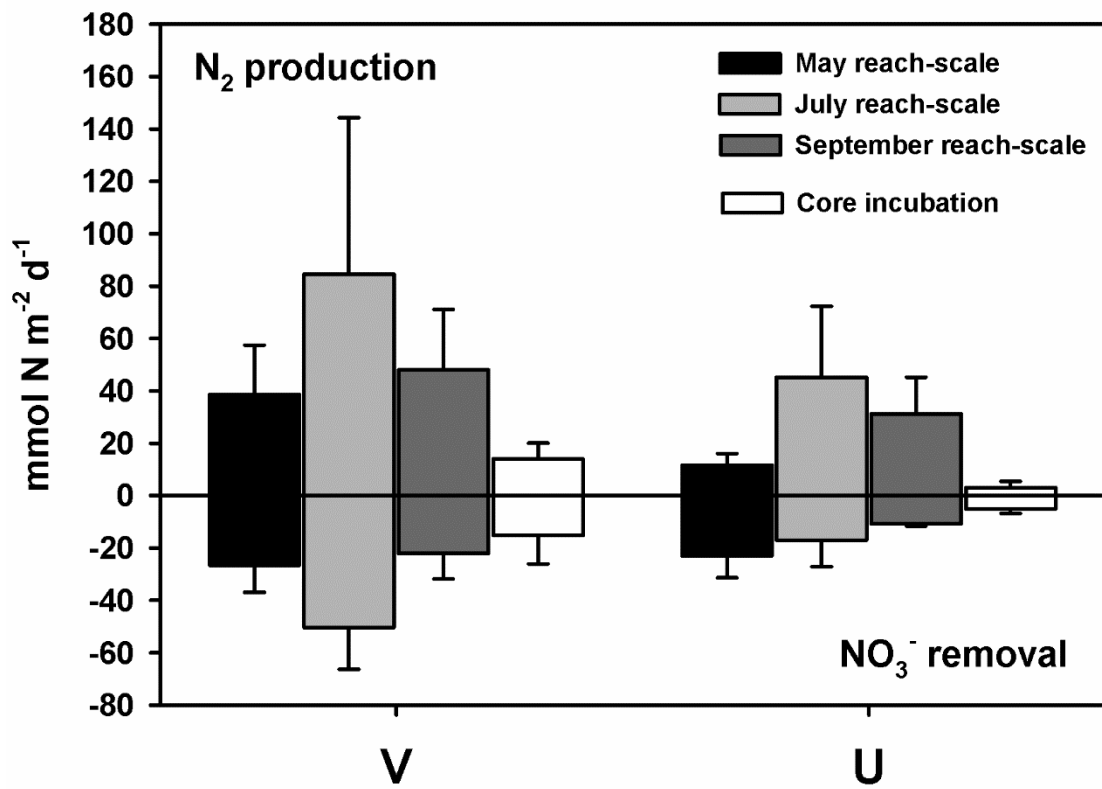


728 \

729 Fig. 2



730  
731 Fig. 3



732 Fig. 4.